

Membrane-Free Osmotic Desalination at Near-room Temperatures Enabled by Thermally-Responsive Polyionic Liquid Hydrogels

Xueyu Yuan^a, Yufeng Cai^{*c}, Jing Jiang^a, Zihao Zhou^a, Chengwei Wang^a, Jinhua Hu^{d,e},
Li Liu^a, Bing Li^a, Ming Liu^{*a,b}

- a. School of Chemistry and Chemical Engineering, Harbin Institute of Technology,
Harbin, 150001, PR China
- b. Engineering Laboratory of Advanced Energy Materials, Ningbo Institute of
Materials Technology & Engineering, Chinese Academy of Sciences, Ningbo
315201, China
- c. State Key Laboratory of Special Functional Waterproof Materials, Beijing
Oriental Yuhong Waterproof Technology Co. Ltd, Beijing 101111, China
- d. State Key Laboratory of Food Science and Technology, Jiangnan University,
Wuxi 214122, China
- e. School of Food Science and Technology, Jiangnan University, Wuxi 214122,
China

Materials and Methods

Materials: Tripentylamine (mixture of branched-chain isomers), and Tripropylamine were commercially available from TCI and used without further purification. 4-chloromethyl styrene, acetonitrile, and diethyl ether were commercially available from Aladdin. 2,2-azobis (2-methylpronamidine) dihy, poly (ethylene glycol) dimethacrylate (PEGDM) were purchased from Sigma-Aldrich. Deionized water was used for all the experiments.

Preparation of N_{555VB}Cl IL monomer: N_{555VB}Cl was prepared according to a method reported elsewhere.^[1] Tripentylamine (12.8 g, 54 mmol) was added to a solution of 4-chloromethyl styrene (10.1g, 60 mmol) in acetonitrile (50 mL) under a nitrogen atmosphere. The mixture was stirred and refluxed for 24 h. After the removal of acetonitrile, the crude product was washed with diethyl ether several times and dried in a vacuum at room temperature to obtain N_{555VB}Cl (12.0 g, 52 % yield) as a white solid.

Preparation of N_{333VB}Cl IL monomer: Tripropylamine (16 g) was added to a solution of 4-chloromethylstyrene (10.1 g) in acetonitrile (50 mL) under a nitrogen atmosphere. Post-treatment of N_{333VB}Cl (15 g, 57% yield) was consistent with N_{555VB}Cl. The structures of IL monomers prepared in this study are shown in Figure 1.

The preparation of PNCl-1 hydrogel: PNCl-1 gel was prepared by combining N_{555VB}Cl monomer, 2,2-azobis (2-methylpronamidine) dihydrochloride, and PEGDM at a molar ratio of 100: 1: 0.1 and 100: 1: 0.2. First, the N_{555VB}Cl monomer was mixed with water (water content: 20 wt%) and PEGDM, and degassed by sonication.

Subsequently, 2,2-azobis (2-methylpronamide) dihydrochloride was added under an N_2 atmosphere and the mixture was transferred into a vial. The vial was sealed and heated at 60 °C for 6 h. The resulting TPIL gel was soaked in deionized water at 1 °C for at least 2 days to remove residual monomer and was completely dried for subsequent studies.

The preparation of PNCl-2 hydrogel: The $N_{555VB}Cl$ and $N_{333VB}Cl$ monomers were mixed at a mass ratio of 95:5, 90:10, and 80:20, followed by mixing with water (water content: 20 wt%) and PEGDM. The 2,2-azobis (2-methylpronamide) dihydrochloride was added under the N_2 atmosphere. Post-treatment of PNCl-2 gel was consistent with the PNCl-1 gel described above.

The preparation of MXene/IL gel: The $N_{555VB}Cl$ and $N_{333VB}Cl$ monomer at a mass ratio of 95:5 was mixed with $Ti_3C_2T_x$ MXene (1, 3, 5 mg mL⁻¹), water (water content: 20 wt%) and PEGDM. The 2,2-azobis (2-methylpronamide) dihydrochloride was added under the N_2 atmosphere. Post-treatment of MXene/IL hybrid gel was consistent with PNCl-1 gel.

Characterization: Scanning electron microscopy (SEM, Quanta 200, FEI, US), operating at 15 kV, and Energy-dispersive X-ray spectroscopy (EDX) were used to analyze the morphologies and element content of the as-prepared TPIL gels. X-ray photoelectron spectroscopy (XPS, BIC Corporation, US) and Fourier transform infrared spectroscopy (FT-IR, AVATAR 360, Nicolet, US) were used to analyze the functional groups and elemental contents. The XPS test employs Al $K\alpha$ ray, and the incident photoelectron energy is 1486.6 eV. With photochemical reagent potassium

bromide as a reference, the as-prepared gels were scanned between 400 and 4000 cm^{-1} at a test rate of 4 cm^{-1} . The water contact angle was measured by the OCA20 machine (Data-physics). The UV-vis-NIR spectra were obtained by a UV-Vis-NIR spectrophotometer (Agilent Cary 5000). Temperature profiles and thermal images of the samples were recorded by a Testo 869 infrared camera. The one-sun solar irradiation was provided by a CEL-S500 Solar Simulator. The concentration of ions of the treated water collected from swelling PNCI gel was tracked by ICP-OES (Thermo, Icap 7400). The salt rejection was determined by the equation, $(1-(C_m/C_o)) \times 100\%$, where C_m is the measured ion concentration and C_o is the original ion concentration in aq. solution. A thermogravimetric analyzer (TGA) was utilized to test the MXene/IL gel samples. All the samples were dehydrated at 120 °C before TGA tests. TOC of the freshwater was measured by TOC-L.

The measurement of swelling degree: we have prepared PNCl-1 and PNCl-2 hydrogels, and their swelling degree has been evaluated after immersing the TPIL gels in aq. NaCl solution (1 L). with different NaCl concentrations at 1.0 °C for 48 h. Then, the TPIL hydrogels were immersed in different aq. NaCl soln. (75 to 600 mmol L⁻¹), and subsequently heated up to the selected temperature (1-80 °C) and kept them for 10 min. The TPILs gels after soaking in pure water or aq. NaCl solutions were calculated by the following equation:

$$\text{Swelling degree (g/g)} = (W_{\text{water}} - W_{\text{dry}}) / W_{\text{dry}}$$

W_{water} : the weight of water-saturated gel; W_{dry} : the weight of fully dehydrated dry gel.

Rejection of NaCl: With ICP OES tests, we measured the concentration of Na⁺ in salt water (600, 300, 150, 75 mmol L⁻¹ NaCl) obtained from PNCl-2 hydrogels. Firstly, PNCl-2 hydrogels were soaked separately in different concentrations of NaCl for 12 h. Then, the gel surface was quickly cleaned with water of 60 °C and wiped off with clear paper, and the water generated under simulated sunlight was collected to test.

Rejection of KCl, Na₂SO₄, NaHCO₃: With ICP OES tests, we measured the concentration of K⁺ in 600 mmol L⁻¹ KCl, Na⁺ in 300 mmol L⁻¹ Na₂SO₄, and Na⁺ in 300 mmol L⁻¹ NaHCO₃ obtained from PNCl-2 hydrogels. Firstly, PNCl-2 hydrogel was soaked in the solution for 12 h. The gel surface was quickly cleaned with water of 60 °C. Then, wipe it off with clear paper, and the water generated under simulated sunlight was collected to test.

The measurement of the concentration of Cl⁻ in the PNCI-2 hydrogel. The concentration of counterions within the P_{555-333VB}Cl hydrogel was estimated to be ~ 2.12 M by assuming all the confined counterions are dissociated.

Calculation of mass loss: With regards to efficient water production for potential practical application, the repeatability of the mass loss of hydrogels should be taken into consideration. To begin with, three pieces of MXene/IL hydrogels prepared separately under the same conditions were placed in 600 mmol L⁻¹ salt water and let to reach the saturation state. The gels were placed under artificial one-sun illumination to induce phase change and hence water release. The water collected was weighed at different time interval.

Calculation of water collection efficiency: To measure the water collection efficiency, the swollen MXene/IL gel was exposed to simulated sunlight with a radiation intensity of 1 kW m⁻² (one sun, 300 W xenon arc lamp) in the air at an ambient temperature of 25 °C. Temperature variation of the MXene/IL hydrogel was measured by using a thermometer at each time interval. Simultaneously, PNCI-1 and PNCI-2 hydrogels and their temperature were evaluated under the same condition. The mass change of TPIL hydrogels was recorded by an electronic mass balance at various times. Because of the hydrophilicity switching of ionic gels and the heating effect of MXene, the weight loss over the entire process was due to water release.

Water collection from salt water: The clean water collection process was carried out by immersing TPIL hydrogels in the salt water (600, 300, 150, 75 mmol L⁻¹ NaCl) for 48 h separately, and then the swelled TPIL hydrogels were taken out and irradiated

with sunlight to generate clean water.

The differential scanning calorimeter (DSC): The LCST of gels was measured by a differential scanning calorimeter (DSC). All gels were put in water to reach the equilibrium state and dry excess water was with filter paper before measurement. TPIL gels (≈ 30 mg) were then loaded in aluminum cells and sealed hermetically. The thermal analysis was performed in a temperature range of 20 – 60 °C with a heating rate of 3 °C min⁻¹ in a dry N₂ atmosphere. However, since there was no endothermic and exothermic peak in the spectrogram tested by DSC, rheological tests and changes in gel transparency were used to characterize the phase transition process in Figure 1 i, j.

Rejection obtained by electrical resistance:

$$\text{Rejection} = \frac{R1 - R2}{R1} \quad (\text{S1})$$

Where R1 and R2 denote the electrical resistance of the elute recovered from PNC1-2 hydrogel with DC=0.2% (1.428 MΩ), 600 mmol/L aq. NaCl solution (0.310 MΩ).

Rejection calculated by Donnan approximation:

$$C_s^g = \left[\left(\frac{\alpha C_{pol}}{2} \right)^2 + (C_s^b)^2 \right]^{\frac{1}{2}} - \frac{\alpha C_{pol}}{2} \quad (\text{S2})$$

where C_s^g , C_{pol} , and α denote the salt concentration of gel, the polymer concentration, and the fraction of charge monomers inside the gel.

$$\text{Rejection} = (C_s^b - C_s^g) / C_s^b$$

$$C = \exp \left(- \frac{C_{pol}}{2C_s^g + \alpha C_{pol}} \frac{6\alpha^2 N \lambda_B}{\kappa R_0^2 (1 + \xi)} \right) \quad (\text{S3})$$

where N , λ_B , R_0 , K , ξ denote the number of monomer units connecting two junctions, the end-to-end distance of a free chain in solution, the inverse Debye screening length, and the parameter ξ are used to simplify the notation [2].

Absorption spectra of MXene/IL gel: MXene/IL gel were recorded with UV-vis-NIR spectrophotometer equipped with an integrating sphere.

$$A\% = 1 - T\% - R\% \quad (S4)$$

Where A represents absorption, T represents transmittance, R represents reflectivity.

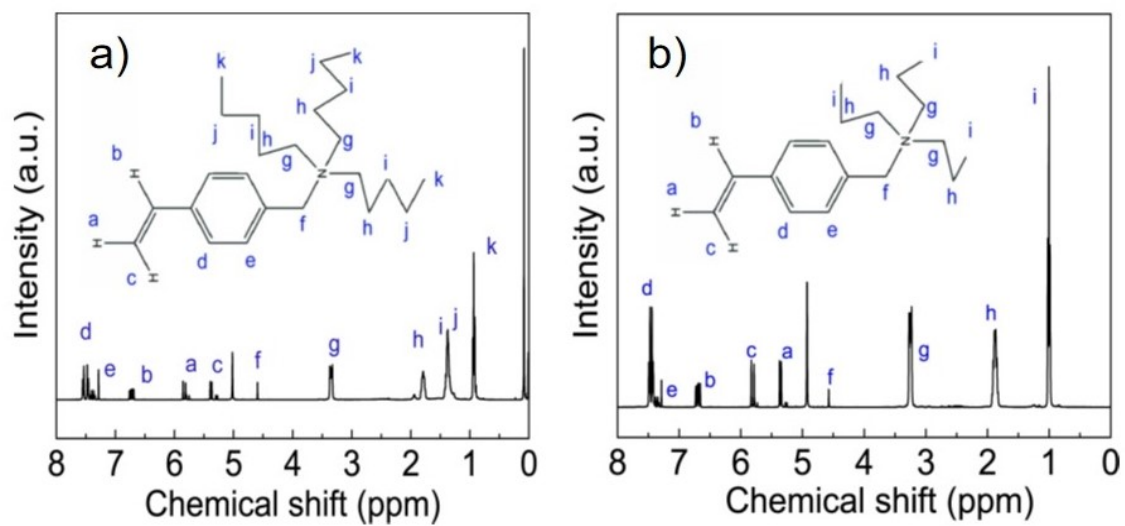


Fig. S1 ^1H NMR spectra of a) $\text{N}_{555}\text{vBCl}$, b) $\text{N}_{333}\text{vBCl}$.

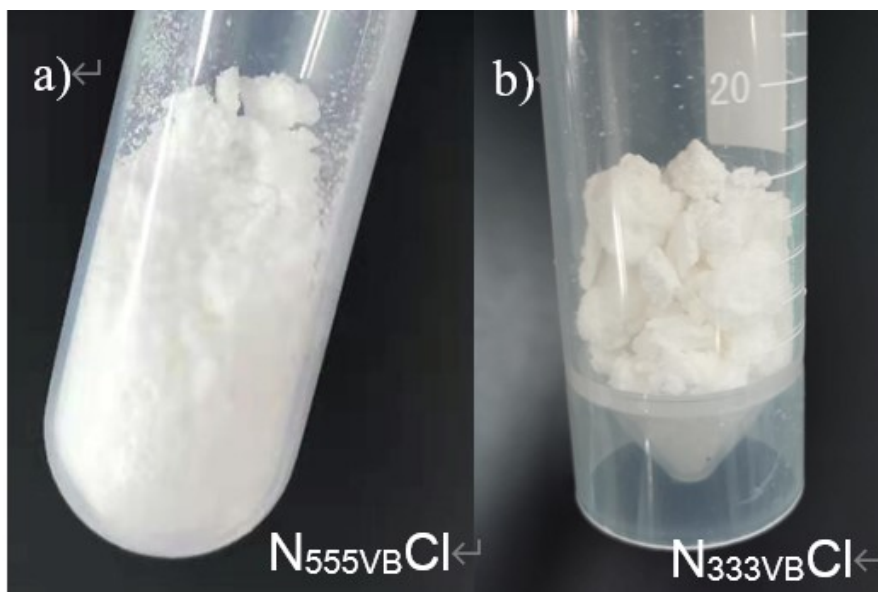


Fig. S2 Photographs of a) N₅₅₅VBCl, b) N₃₃₃VBCl.

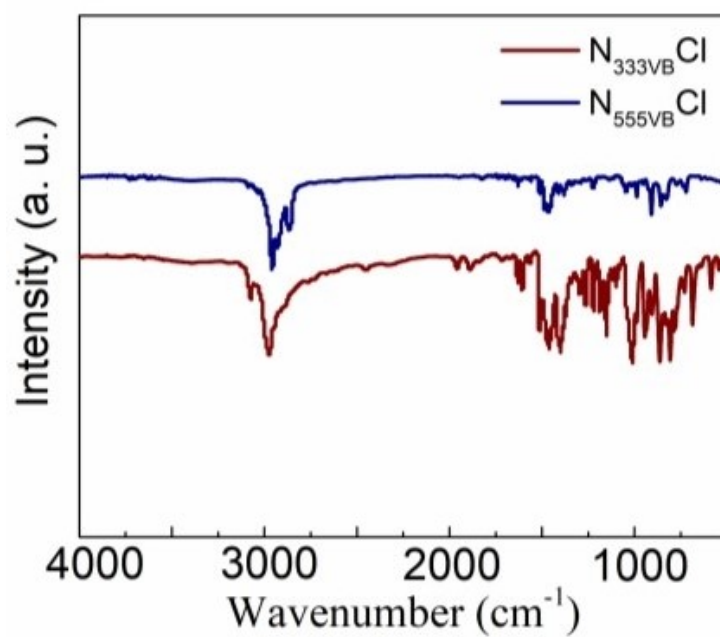


Fig. S3 FTIR of N_{555VB}Cl and N_{333VB}Cl monomer.

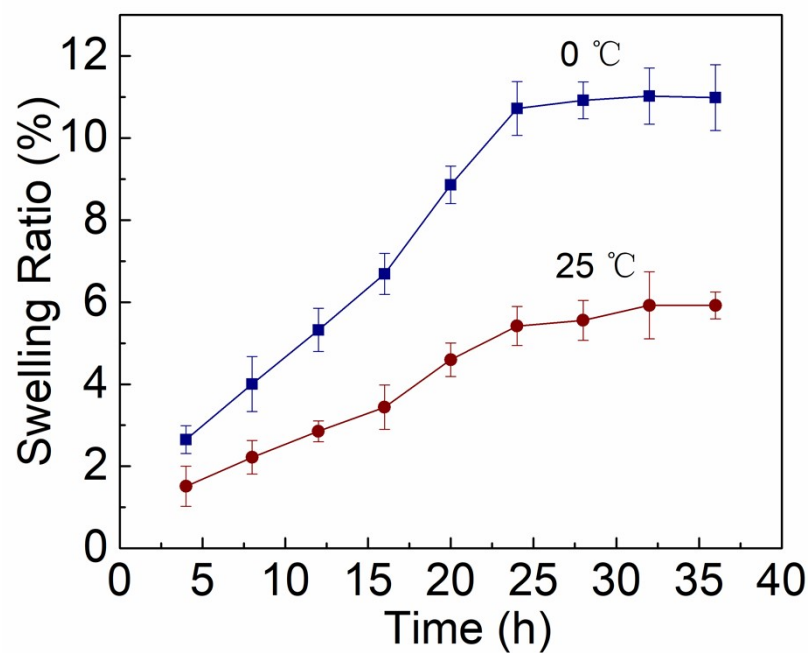


Fig. S4 The compression curves of PNCI-2 hydrogel.

The PNCI-2 hydrogel can better absorb water at 0 °C than 25 °C. The hydrogel would reach saturation after soaking in 600 mmol L⁻¹ saline for 24 h.

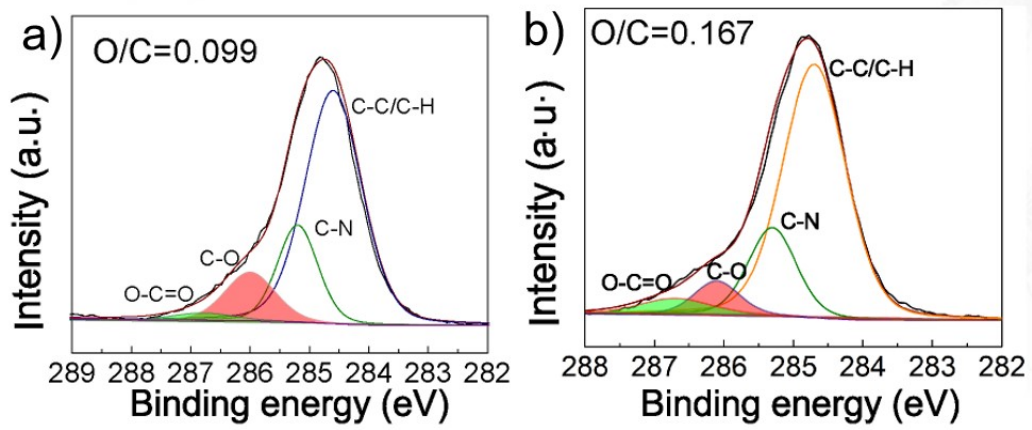


Fig. S5 XPS spectra of e) PNCl-1 hydrogel, f) PNCl-2 hydrogel.

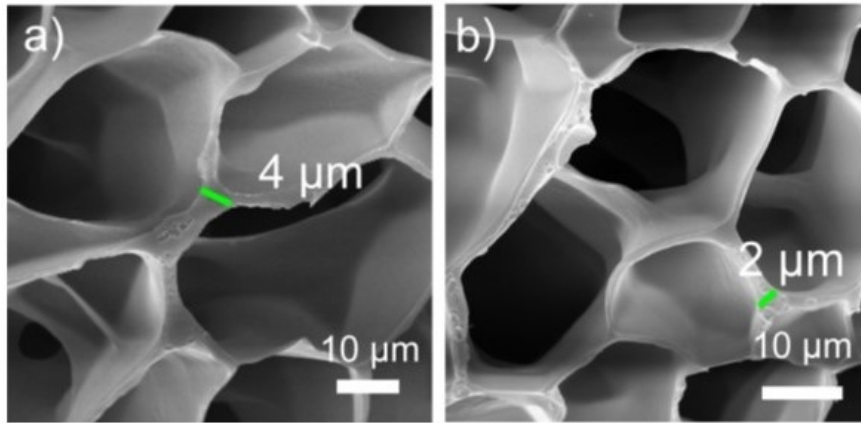


Fig. S6 SEM images of a) PNCl-1hydrogel, and b) PNCl-2 hydrogel.

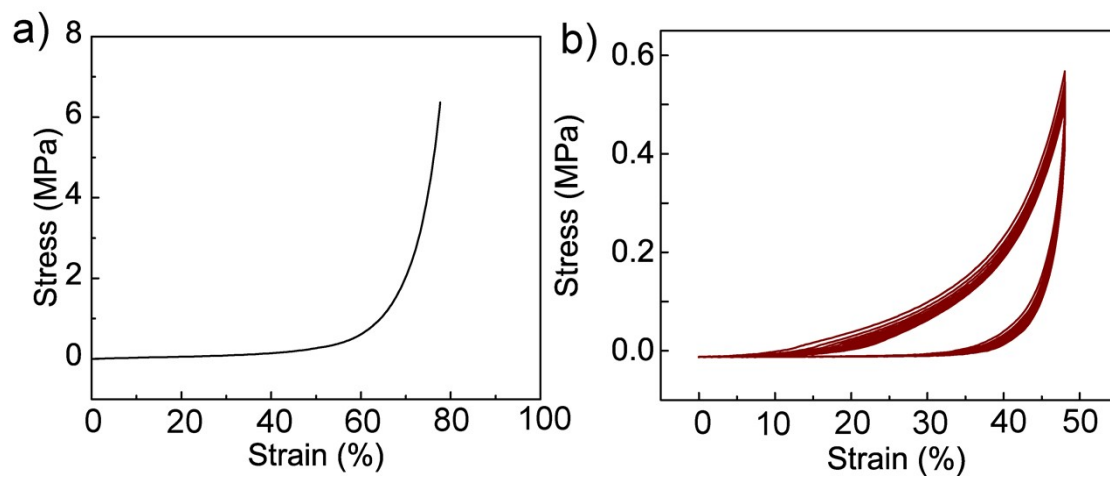


Fig. S7 The compression curves of PNCl-2 hydrogel.

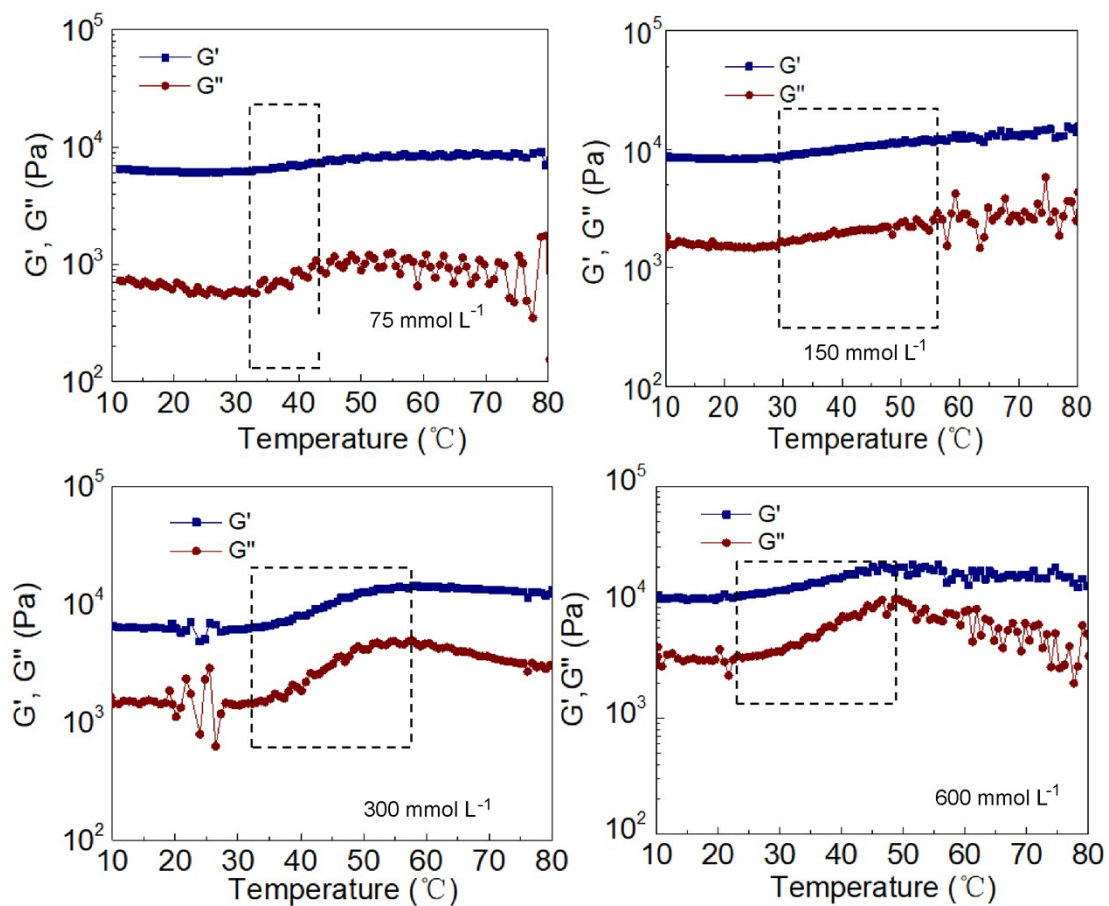


Fig. S8 The variation of G' and G'' as a function of temperature for PNCl-2 hydrogel immersed in 75-600 mmol L⁻¹ NaCl solutions.

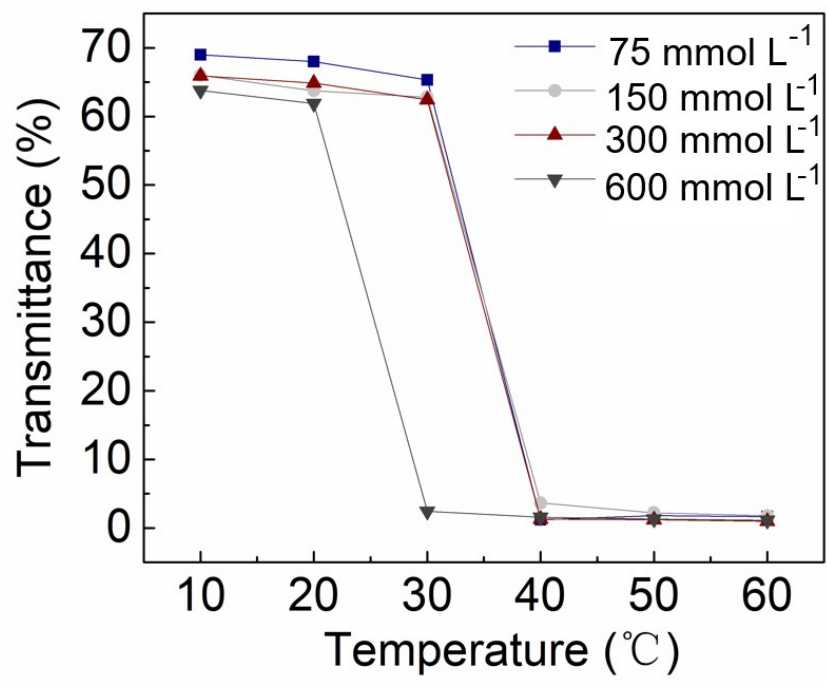


Fig. S9 The variation of transmittance as a function of temperature for PNCl-2 hydrogel.

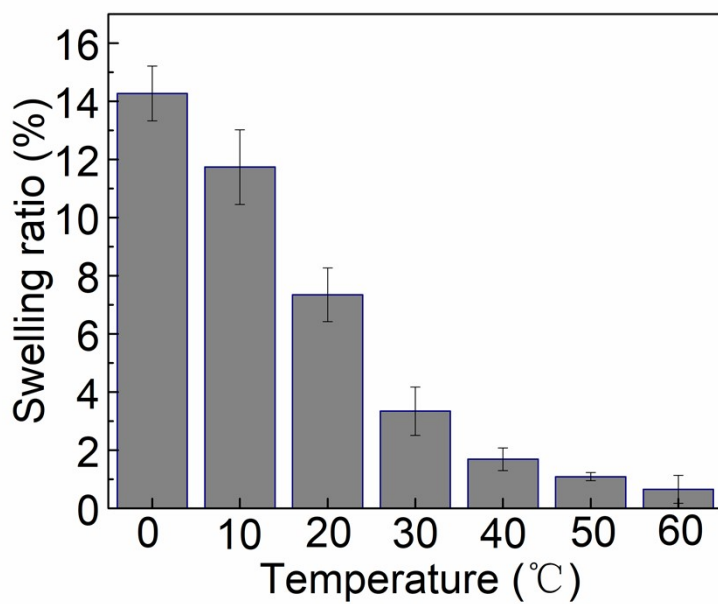


Fig. S10 Swelling degree of PNCl-2 with DC=0.1% in 600 mmol/L NaCl solution.

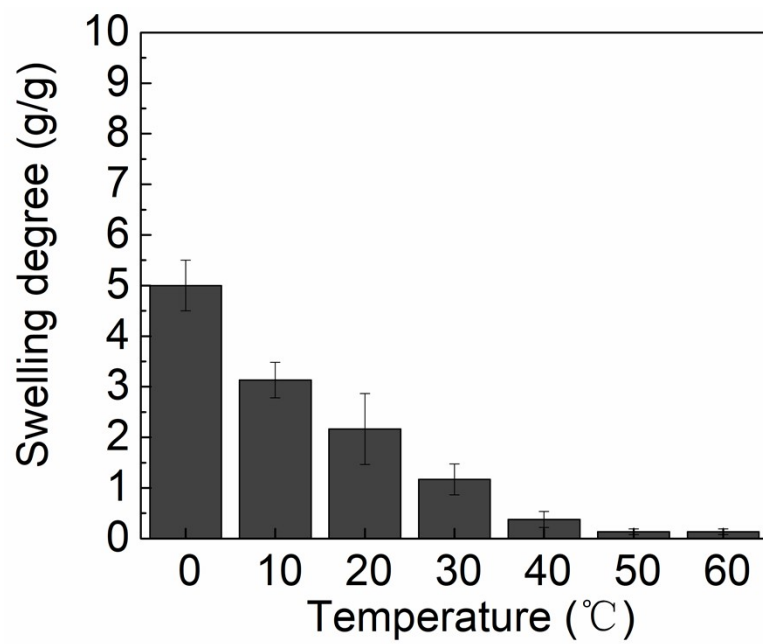


Fig. S11 Swelling degree of PNCl-2 with DC=0.3% in 600 mmol/L NaCl solution.

Table S1 The atoms percentage (C, Cl, N, O) of PNCI-1gel, PNCI-2gel.

The type of gel	Atom percentage of C (%)	Atom percentage of Cl (%)	Atom percentage of N (%)	Atom percentage of O (%)
PNCI-1gel	89.60	3.17	4.28	2.95
PNCI-2gel	87.68	3.90	5.82	2.61

Table S2 The weight percentage (C, Cl, N, O) of PNCI-1gel, and PNCI-2gel.

The type of gel	The weight percentage of C (%)	The weight percentage of Cl (%)	The weight percentage of N (%)	The weight percentage of O (%)
PNCI-1gel	83.06	8.67	4.62	3.65
PNCI-2gel	80.12	10.51	6.20	3.17

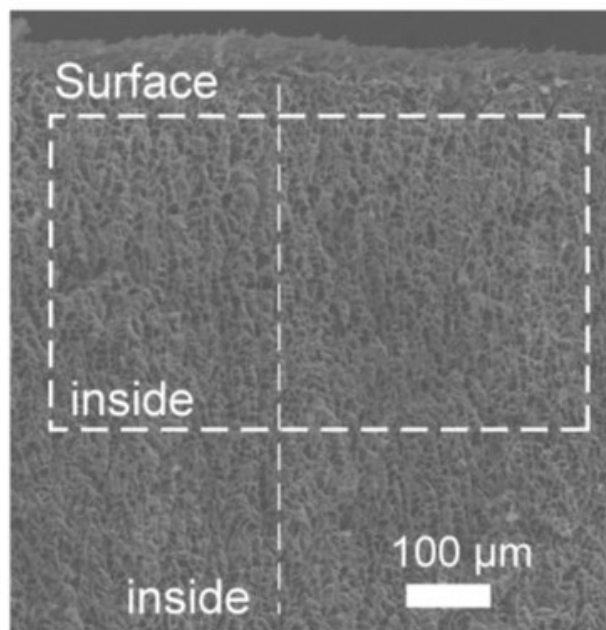


Fig. S12 SEM images of PNCl-2 hydrogel after immersion in 600 mmol L⁻¹ NaCl.

It presents the area range of the mapping from the surface to the interior of the PNCl-2 hydrogel gel.

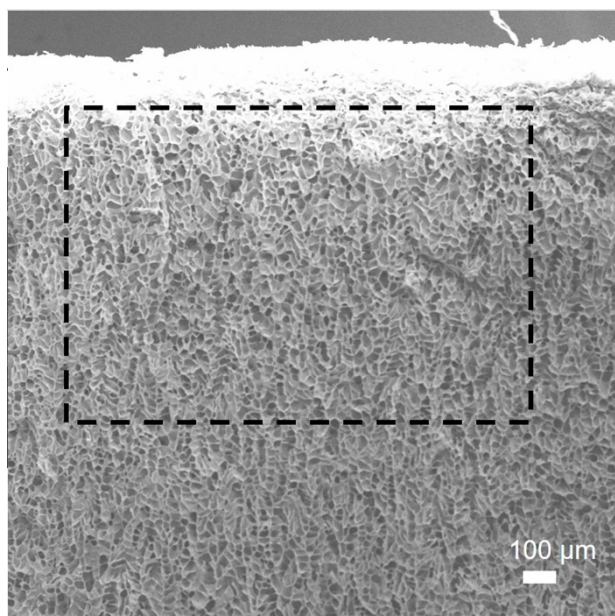


Fig. S13 SEM images of PNCl-2 hydrogel after immersion in 300 mmol L⁻¹ Na₂SO₄.

It presents the area range of the mapping from the surface to the interior of the PNCl-2 hydrogel.

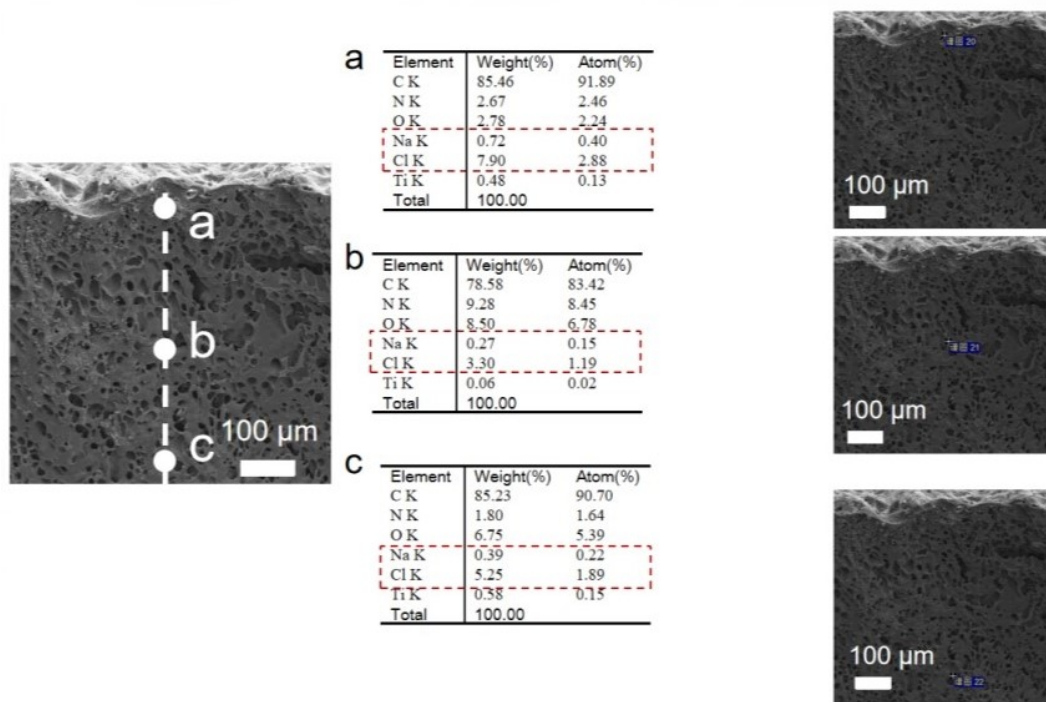


Fig. S14 SEM images and EDX of TPIL hydrogel after immersion in 600 mmol L⁻¹ NaCl.

It presents the SEM images from the top to the bottom of the TPIL hydrogel after immersion in 600 mmol L⁻¹ NaCl. Elemental-distribution mapping with energy-dispersive X-ray spectrometry (EDX) reveals the element content (C, N, O, Ti, Cl, Na) of the three-point separately. As seen, the atomic content of Na and Cl in point b is significantly lower than that in points a and c on the surface.

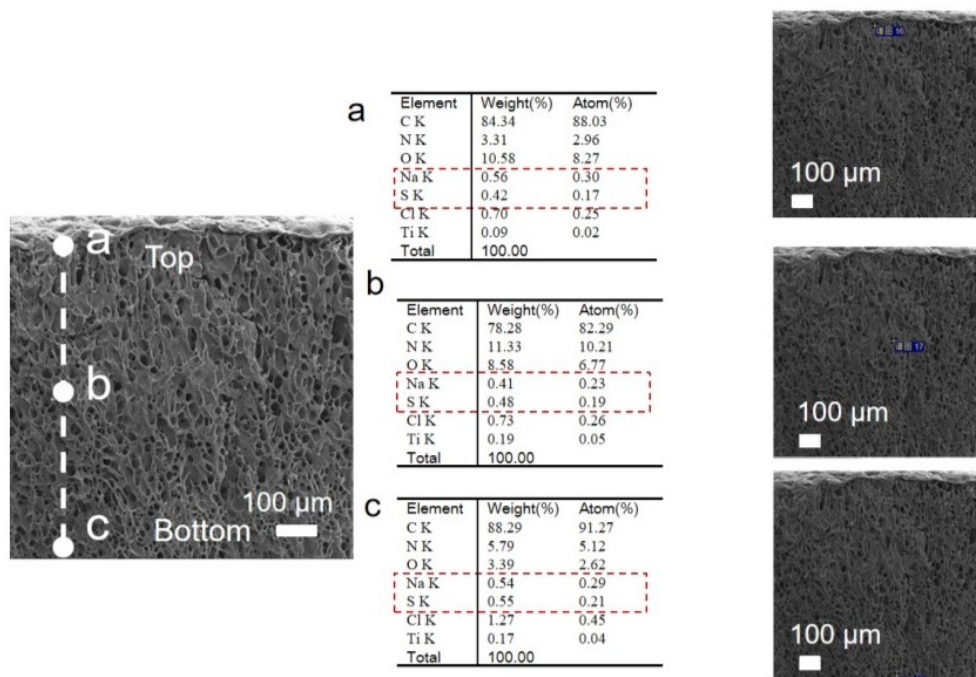


Fig. S15 SEM images and EDX of TPIL hydrogel after immersion in 300 mmol L⁻¹ Na₂SO₄.

It presents the SEM images from the top to the bottom of the TPIL hydrogel after immersion in 300 mmol L⁻¹ Na₂SO₄. Elemental-distribution mapping with energy-dispersive X-ray spectrometry (EDX) reveals the element content (C, N, O, Ti, Cl, Na) of the three-point separately. As seen, the atomic content of Na and S in point b is not much different from that in points a and c on the surface.

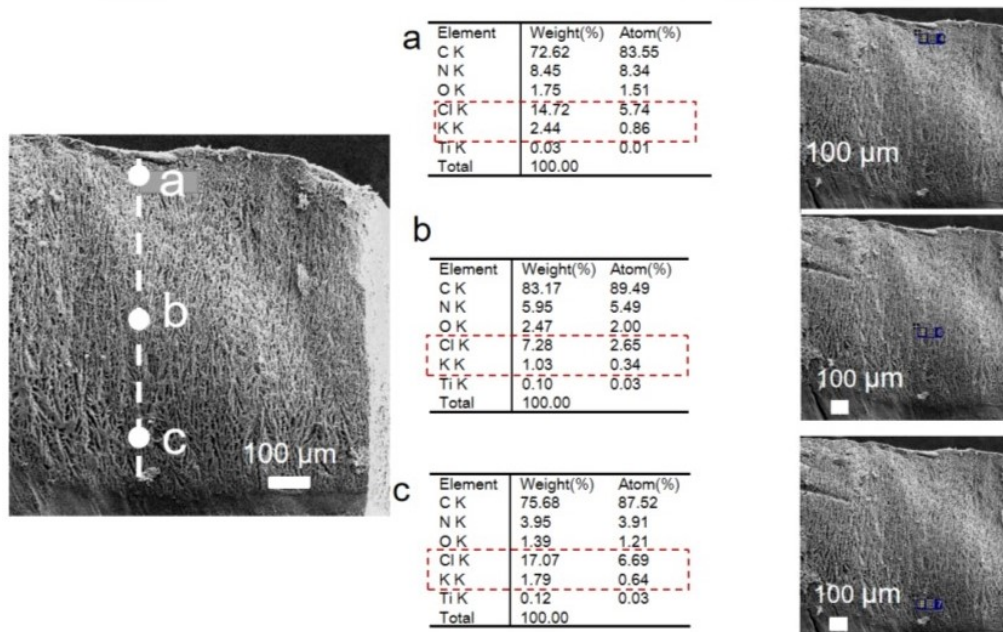


Fig. S16 SEM images and EDX of TPIL hydrogel after immersion in 600 mmol/L KCl.

It presents the SEM images from the top to the bottom of the TPIL hydrogel after immersion in 600 mmol L⁻¹ KCl. Elemental-distribution mapping with energy-dispersive X-ray spectrometry (EDX) reveals the element content (C, N, O, Ti, Cl, K) of the three-point separately. As seen, the atomic content of K and Cl in point b is significantly lower than that in points a and c on the surface.

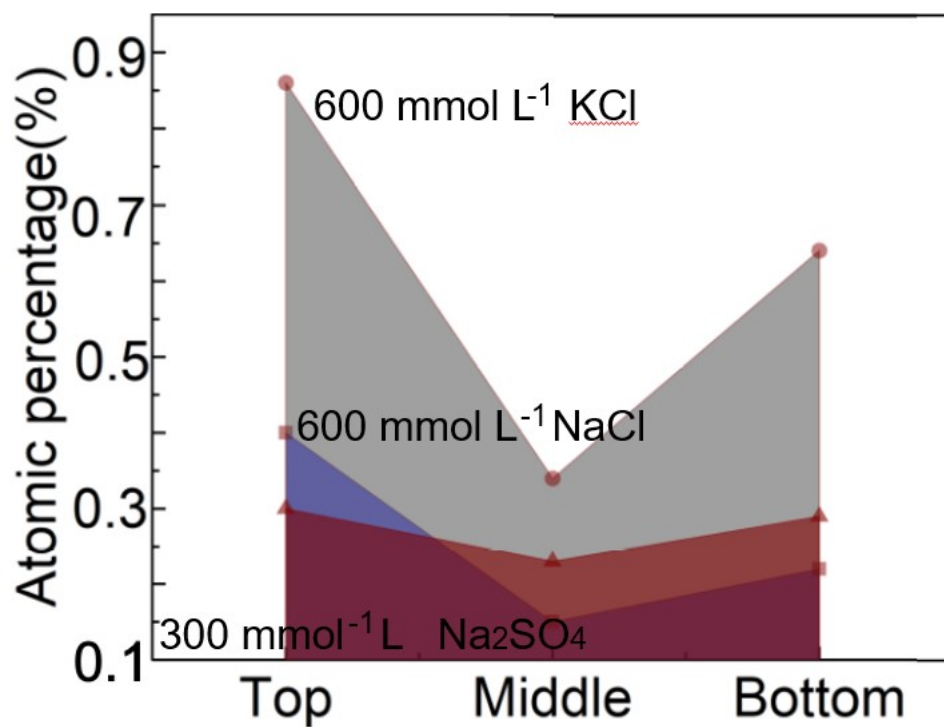


Fig. S17 The variation of atomic percentage of TPIL hydrogel soaked in 600 mmol L⁻¹ NaCl, KCl, and 300 mmol/L Na₂SO₄ from top to bottom.

The atomic content of Na⁺ and K⁺ in NaCl and KCl in point b is significantly lower than that in points a and c on the surface. The atomic content of Na⁺ in Na₂SO₄ in point b is not much different from that in points a and c on the surface.

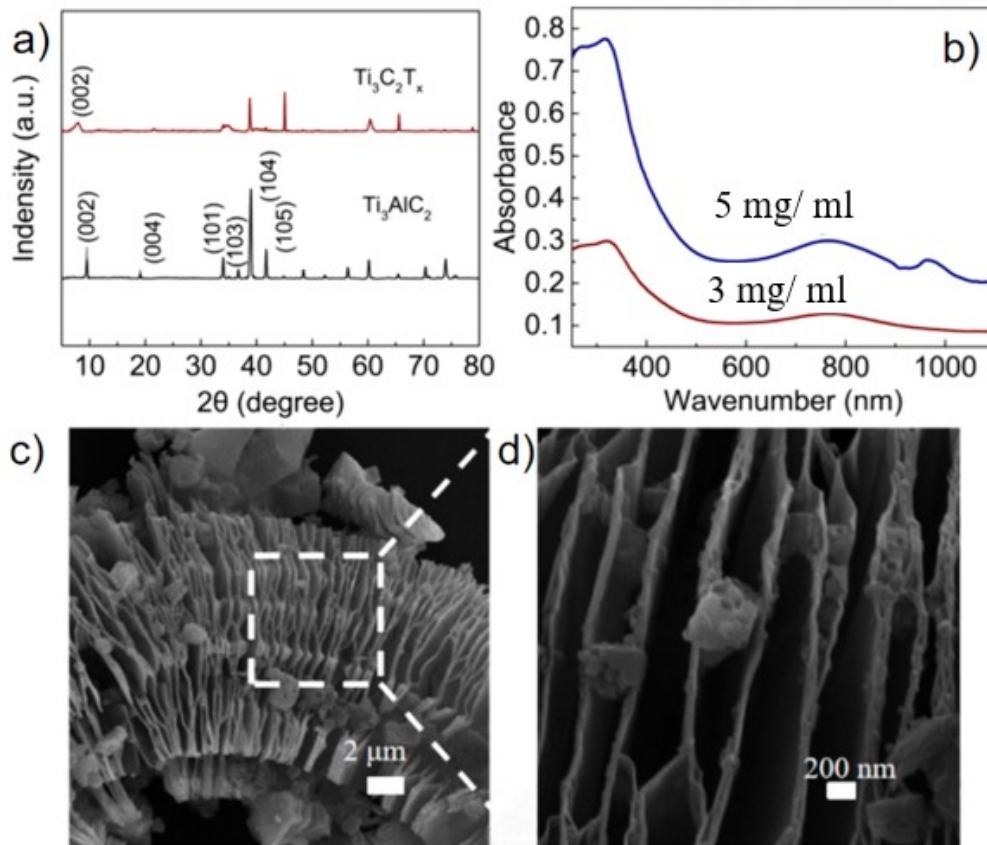


Fig. S18 The characterization of $\text{Ti}_3\text{C}_2\text{T}_x$ MXene. a) X-ray diffraction (XRD) peak showing shifts of the (002) peak and the attenuation of (101), (103), (104), (105) due to the etching of the Al layer. b) UV-vis-NIR absorbance spectra of MXene (3, 5 mg ml⁻¹). c, d) The SEM morphology of $\text{Ti}_3\text{C}_2\text{T}_x$ MXene.

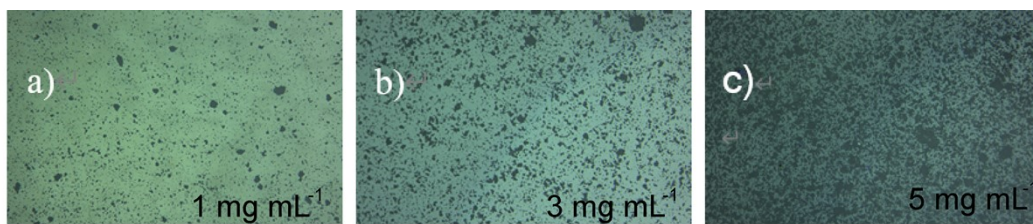


Fig. S19 The distribution of MXene in gels with different concentrations was observed by an optical microscope. a) 1 mg mL^{-1} MXene, b) 2 mg mL^{-1} MXene, c) 5 mg mL^{-1} .

The distribution of different concentrations of MXene in the gels changed from sparse to agglomerated, and the distribution of 3 mg mL^{-1} MXene is uniform.

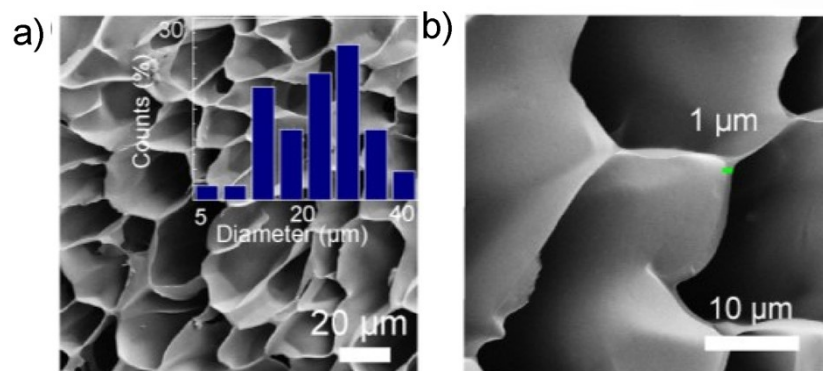


Fig. S20 a, b) The morphology of $\text{Ti}_3\text{C}_2\text{T}_x$, MXene/IL hydrogels, and high-resolution image of MXene/IL gels.

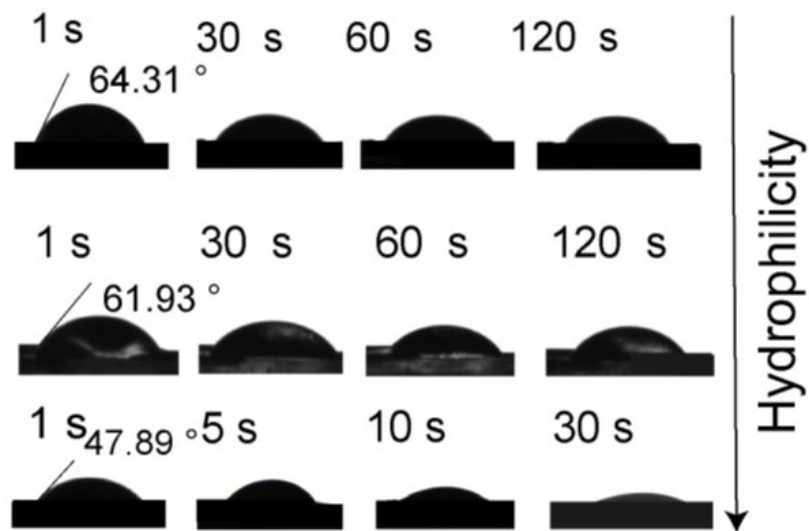


Fig. S21 Optical images showing the dynamic wetting behaviors of a water droplet atop PNCl-1 hydrogel (top), PNCl-2 hydrogel (middle), and MXene/IL composite gel (bottom) at room temperature, as a function of time.

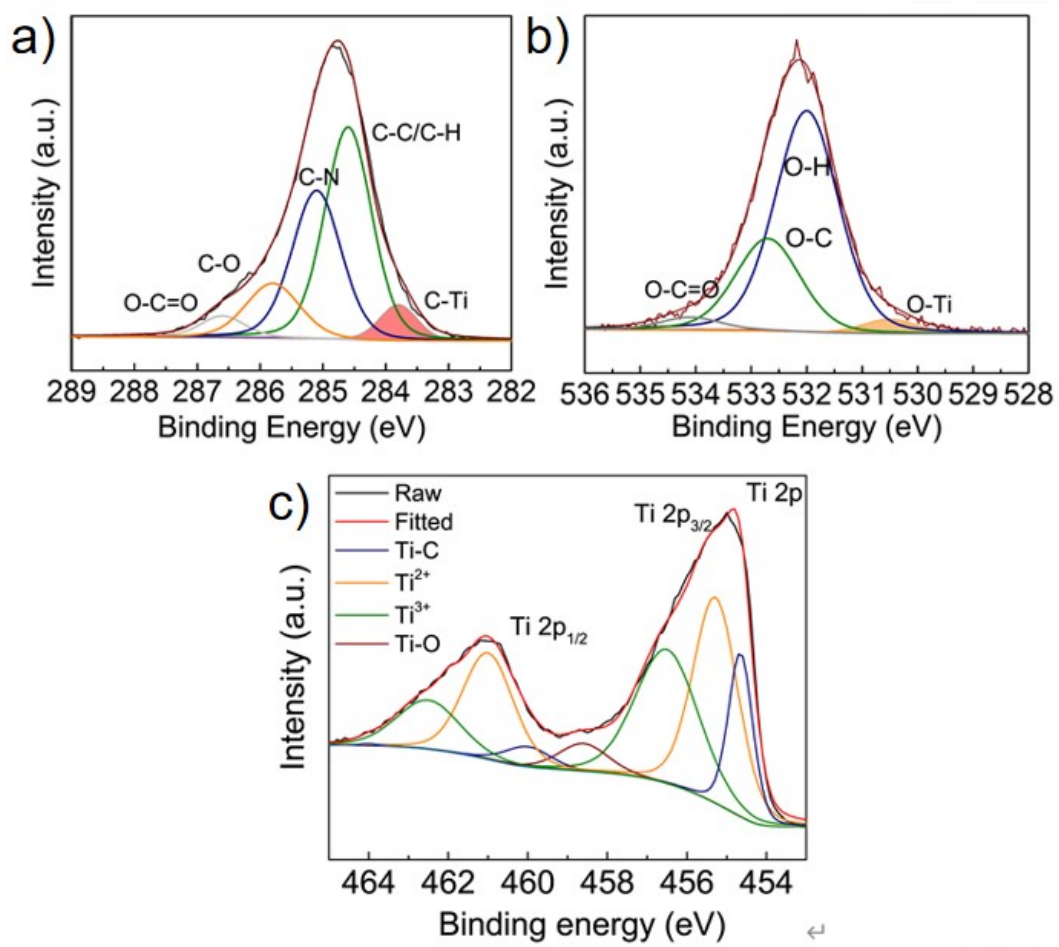


Fig. S22 XPS spectra data of a) C 1s, b) O 1s, c) Ti 2p of MXene/IL gel

As seen in **Figure S20** The MXene/IL gel has stronger C-O and O-C=O peaks and appears C-Ti, O-Ti, Ti-C, and Ti-O peaks, which results from the successful introduction of hydrophilic MXene.

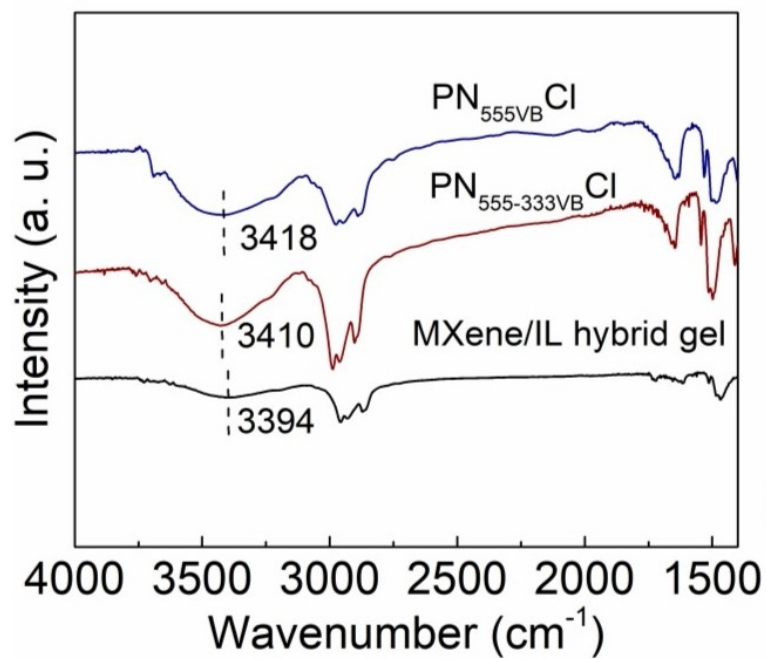


Fig. S23 FTIR of PNCl-2 hydrogel and MXene/IL hydrogel.

The peak for stretching vibration of -OH is red-shifted from 3418 cm⁻¹ for the PNCl-1gel to 3394 cm⁻¹ for the weakened absorption peak of MXene/IL hydrogel, demonstrating the hydrogen bonding between IL monomer and MXene nanosheets.

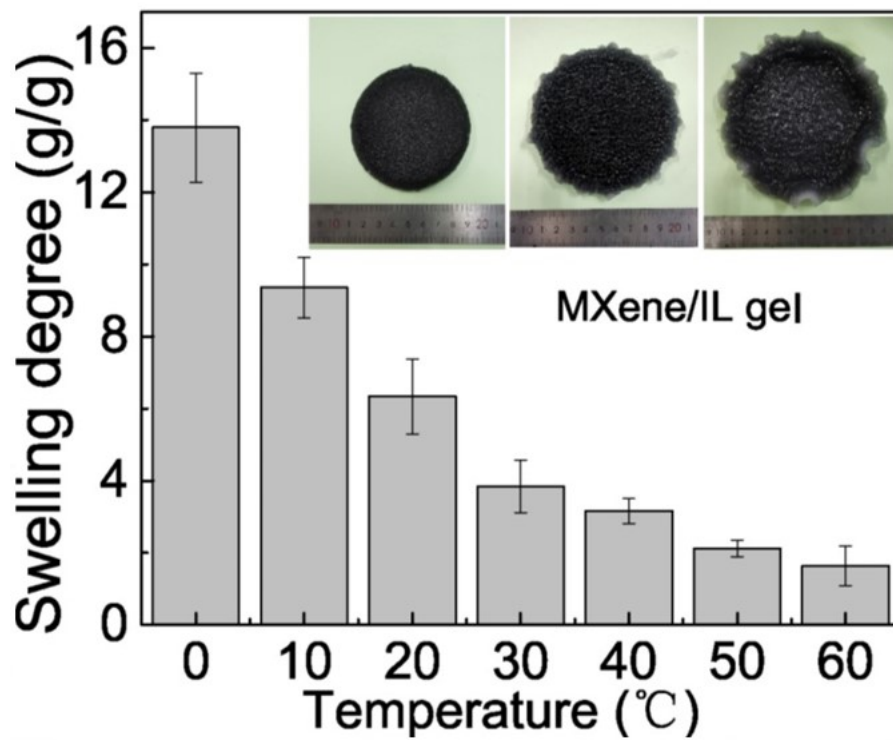


Fig. S24 Swelling degree of MXene/IL hydrogel immersed in 600 mmol L⁻¹ NaCl as a function of temperature.

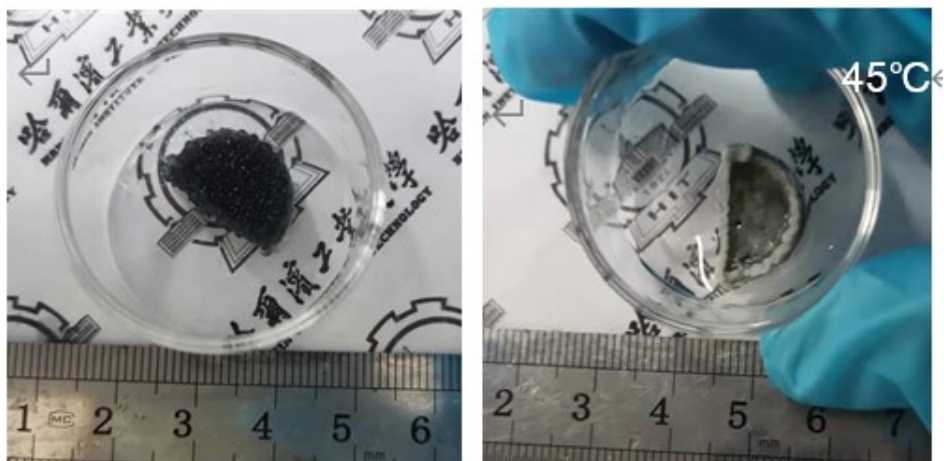


Fig. S25 Photographs of a) MXene/IL hydrogel at room temperature, b) MXene/IL hydrogel after heating.

The TPIL hydrogels after the addition of MXene will not affect the phase transition to release water.

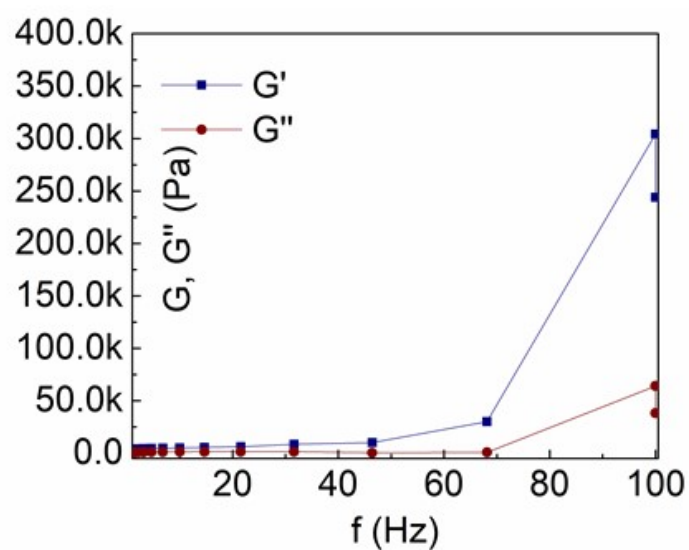


Fig. S26 The G' and G'' vary with frequency for MXene/IL hydrogel.

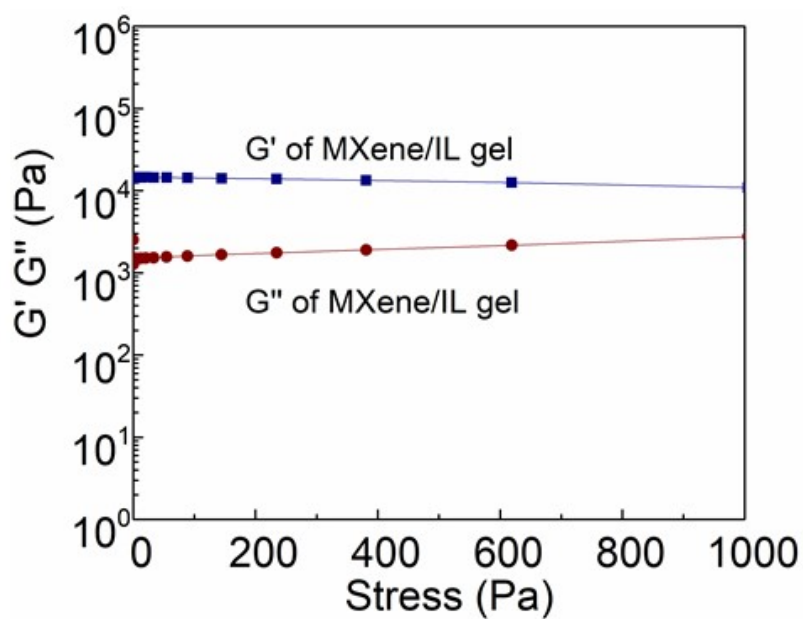


Fig. S27 Storage modulus (G') and loss modulus (G'') as functions of stress for MXene/IL hydrogel

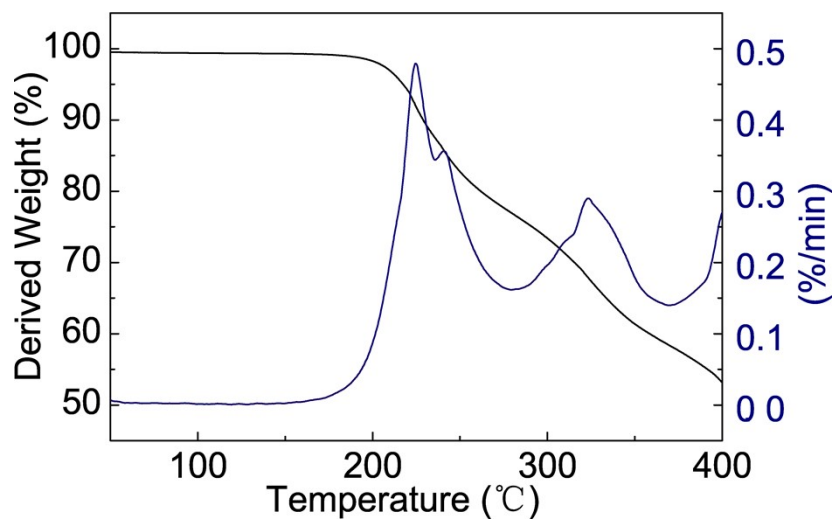


Fig. S28 The TG and DTG curves of MXene/IL hydrogel.

Reference

- 1 T. Richter, J. Landsgesell, P. Košovan, C. Holm, *Desalination*, 2017, **414**, 28.